Research article

Lasers and materials in selective laser sintering

J.P. Kruth
X. Wang
T. Laoui and
L. Froyen

The authors

J.P. Kruth, **X. Wang**, **T. Laoui** and **L. Froyen** are all based at the Catholic University of Leuven, Celestijnenlaan, 300B, Leuven, B-3001, Belgium. E-mail: Jean-Pierre.kruth@mech.kuleuven.ac.be

Keywords

Sintering, Lasers, Simulation, Formed materials

Abstract

Selective laser sintering (SLS) is one of the most rapidly growing rapid prototyping techniques (RPT). This is mainly due to its suitability to process almost any material: polymers, metals, ceramics (including foundry sand) and many types of composites. The material should be supplied as powder that may occasionally contain a sacrificial polymer binder that has to be removed (debinded) afterwards. The interaction between the laser beam and the powder material used in SLS is one of the dominant phenomena that defines the feasibility and quality of any SLS process. This paper surveys the current state of SLS in terms of materials and lasers. It describes investigations carried out experimentally and by numerical simulation in order to get insight into laser-material interaction and to control this interaction properly.

Electronic access

The Emerald Research Register for this journal is available at
http://www.emeraldinsight.com/researchregister

The current issue and full text archive of this journal is available at
http://www.emeraldinsight.com/0144-5154.htm

1. Introduction

Selective laser sintering (SLS) is a rapid prototyping process that allows to generate complex 3D parts by solidifying successive layers of powder material on top of each other (Kruth, 1991). Solidification is obtained by fusing or sintering selected areas of the successive powder layers using thermal energy supplied through a laser beam (Figure 1). A beam deflection system (galvano mirrors or XY table (Van der Schueren and Kruth, 1995a) makes the beam scan each layer according to the corresponding cross section of the part as calculated from a CAD model. A powder deposition system (Van der Schueren and Kruth, 1995b) is used for depositing the successive thin layers of powders (typically 0.1-0.3 mm thickness) in a building container before that layer is laser sintered.

Table I illustrates the recent success of SLS which depicts the largest growth in market share since 1997. This growth is expected to proceed, since – unlike other material additive manufacturing processes mentioned in Table I (Kruth, 1991; Kruth *et al.*, 1998a) – hardly no limitation exists to the materials that might be processed by SLS. The relative importance of SLS will further rise as material additive technology will be used for other applications than the sole production of rapid prototypes and will extend to rapid manufacturing of, e.g. moulds and dies (rapid tooling) or other functional parts in an ever wider range of materials.

2. Materials in SLS

SLS can be used to process almost any material, provided it is available as powder and that the powder particles tend to fuse or sinter when heat is applied. This is the case for most materials. Powders that depict low fusion or sintering properties can be laser sintered by adding a sacrificial binder material

This is an updated and edited version of a paper first published in Geiger, M. and Otto, A. (Eds) (2001), "Laser assisted net shape engineering 3", *Proceedings of the LANE 2001 Conference*, 28-31 August 2001, Erlangen, Germany, Meisenbach Bamberg. Many of the research results presented here benefited from financial support of Belgian national fund IUAP P4/33 and Flemish Science Foundation project FWO G.0216.00.

Assembly Automation
Volume 23 · Number 4 · 2003 · pp. 357–371
MCB UP Limited · ISSN 0144-5154

Figure 1 Schematic overview of SLS process

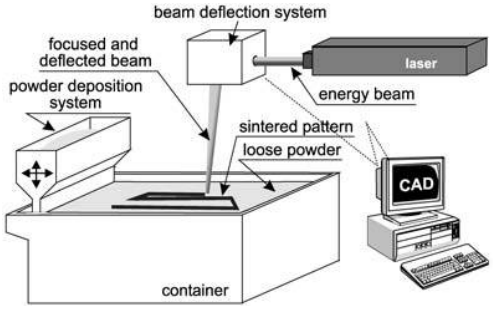

(typically a polymer binder) to the basic powder. After sintering the full part, the sacrificial binder can be removed by debinding the "green" part in a thermal furnace. The use of a sacrificial binder allows to enlarge the pallet of laser sinterable materials. However, the range of materials (powders) that can be laser sintered without sacrificial binder is quite large as compared to other rapid prototyping processes.

2.1 SLS of polymers

Polymer powders were the first and are still the most widely applied materials in SLS (Figure 2).

Amorphous polymers, like polycarbonate (PC) powders, are able to produce parts with very good dimensional accuracy, feature resolution and surface finish (depending on the grain size). However, they are only partially consolidated. As a consequence, these parts are only useful for applications that do not require part strength and durability. Typical applications are SLS masters used for manufacturing silicone rubber and cast epoxy moulds (McAlea *et al.*, 1997).

Semi-crystalline polymers, like nylons (polyamide (PA)), on the contrary, can be sintered to fully dense parts with mechanical properties that approximate those of injection moulded parts. On the other hand, the total SLS process shrinkage of these semi-crystalline polymers is typically 3-4 per cent (Grimm, 1997), which complicates production of accurate parts. The good mechanical properties of these nylon based parts make them particularly suited for high strength functional prototypes. New grades of nylon powders (i.e. Duraform PA12, Schumacher and Levy, 1998) even yield a resolution and surface roughness close to those of PC, making PA also suited for casting silicone rubber and epoxy moulds, even though higher resolutions and smoother surfaces can still be obtained from amorphous powders.

Other polymer-based materials available commercially are acrylic styrene (PMMA/PS) for investment casting and an elastomer for rubber-like applications (Figure 2, top left part).

Table II gives an overview of the mechanical properties of some typical SLS polymer materials supplied by one of the major SLS vendors.

2.2 SLS of reinforced and filled polymers

PA powders can be relatively easily reinforced with other materials in order to further improve their mechanical and thermal properties (Table II). Several grades of glass fibre reinforced PA powders are readily available on the market (Seitz *et al.*, 1997).

PA coated copper powder (Cu-PA) is also available for the production of plastic-metal composite injection tools (Bruning, 1998). This Cu-PA powder mixture contains 70 wt per cent Cu (rest is PA). Compared to plain PA parts (see Table II), Cu-PA SLS parts are 3.5 times heavier (density of 3.45 g/cm^3), four times more thermally conductive (1.28 W/m°C) and exhibit a similar tensile strength (34 MPa), but a higher tensile modulus (3.4 GPa). Applications include Cu-PA inserts for injection moulds. Those Cu-PA moulds can be used as laser sintered without the need for removal of the PA phase or without any post-densification process, while still depicting a life time of 200-400 shots.

Table I RP systems unit sales

Process	Sales in 1999	Difference with 1997 (per cent)
Stereolithography (SL)	291 units (24.4 per cent)	+3.5
Fused deposition mod. (FDM)	293 units (24.5 per cent)	+13
Ink jet printing (IJP)	389 units (32.5 per cent)	+47
Laminated object mfg. (LOM)	94 units (9 per cent)	− 42
SLS	115 units (9.6 per cent)	+53

Figure 2 Polymer parts made by SLS

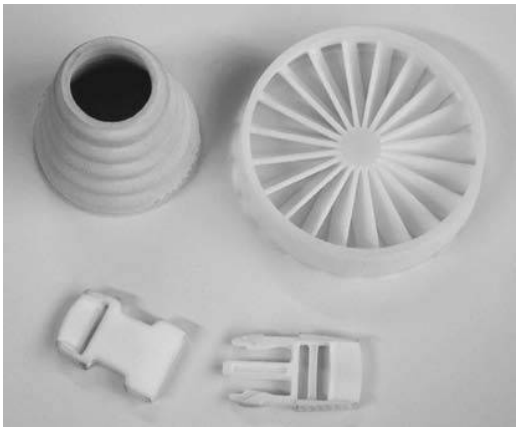

2.3 SLS of metals, hardmetals and cermets

SLS is one of the very few rapid prototyping processes that allow direct manufacturing of metallic components without the use of a polymer binder. Other processes allowing direct production of metallic parts are 3D laser cladding processes (e.g. SDM (Fessler *et al.*, 1998), LENS (Griffith *et al.*, 1996), CMB (Klocke and Clemens, 1996)) and lamination of metal sheets by laser cutting and stacking of sheet material (e.g. LLCC (Dormal *et al.*, 1998), metal sheet lamination (Himmer *et al.*, 1999), CAM-LAM process). Those alternative processes, however, suffer from major limitations in terms of achievable shape complexity and accuracy and are therefore often combined with milling (possibly on a single machine) to remedy those drawbacks. SLS also allows to produce metallic parts using some kind of sacrificial polymer binder, as done with few other RP processes (e.g. SL, 3D printing, LOM). This allows us to further enlarge the range of powders processible by SLS, but requires a furnace post treatment to remove the polymer binder and yield a plain metallic or cermet parts (the so-called debinding). The porosity of laser sintered part may also require a post-densification operation that may be obtained by furnace post-sintering, by pore infiltration with a metallic or polymeric infiltrant material (Behrendt and Shellabear, 1995; Heymadi and McAlea, 1996), or by hot isostatic pressing (Das *et al.*, 1998; Knight *et al.*, 1996). The following sections will distinguish between those SLS processes that apply polymer binders or infiltrants and those that do not.

2.3.1 SLS of metals and cermets with polymer binder or infiltrant

DTM Corporation (Austin, USA) has developed a process that applies polymer-coated steel powders (1080 steel, 316 or 420 stainless steel particles coated/mixed with a thermoplastic/thermoset material) for the SLS of metal parts (Figure 3(a)). During laser sintering, the polymer melts and acts as a binder for the steel particles. After debinding the porous steel part is infiltrated with copper or bronze (McAlea, 2000; McAlea *et al.*, 1997). The resulting material properties are quite close to those of plain steel materials as shown in Table III. Over the years, DTM continuously improved their production process by reducing the number of post-processing cycles and their total duration. For the third generation of RapidSteel powder called LaserForm ST-100, composed of 60 per cent 420 stainless steel and 40 per cent bronze (89Cu-11Sn), debinding and infiltration can be done in a single furnace cycle of about 24 h under pure nitrogen. These developments yield improved material properties of the final SLS parts such as strength, hardness, machinability, weldability, wear rate and thermal conductivity (McAlea, 2000).

Using a similar binder-based SLS process, the University of Texas at Austin produced parts in a SiC-Mg cermet material. It applies SiC particles coated with a proprietary polymer binder to obtain a SiC preform with a typical density of 40 vol per cent (Wohlert and Bourell, 1996). After debinding (at 400°C) the SiC preform becomes quite fragile

Table II Overview of the mechanical properties of some SLS polymer materials (DTM)

	PC	Fine nylon (PA)	Glass filled nylon	Elastomer
E-modulus (MPa)	1200	1,400/1,800[a]	2,800/4,400[a]	20
Tensile strength (MPa)	23	36/44[a]	49/42[a]	–
Break elongation (per cent)	5	6/22[a]	1.8[a]	111
Surface roughness R_a as SLS processed (μm)	7	12/8.5[a]	15	–

Note: [a]Value for DuraForm PA

Figure 3 Plastic injection moulds or inserts made by SLS

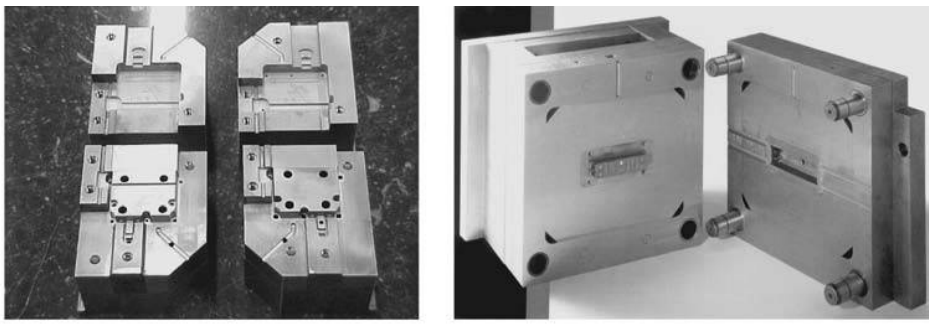

a. Mould inserts made from polymer coated Rapidsteel 2 powder and infiltrated with bronze

b. Mould with inserts made for bronze powder and infiltrated with epoxy

Table III Overview of the mechanical properties of laser sintered metals (after post-processing and infiltration) and of common plain casted steel

	Reference plain casted steel	RapidSteel 2 powder + bronze infiltration (DTM)	LaserForm ST100 + bronze infiltration (DTM)	Steel/Cu-P/Ni powder (EOS)	Bronze/Ni/P powder + epoxy infiltration (EOS)
E-modulus (GPa)	210	193	153	164	92
Yield strength of 0.2 per cent (MPa)	418	329	326	414	168
Tensile strength (MPa)	500	509	587	491	161

preventing further handling. To improve the strength of the SiC preform, an additional firing step (1,100°C, 2 h, formation of SiO_2 layer) was utilized followed by (pressureless) infiltration (670°C) with a Mg-based (AZ91D) die casting alloy (Wohlert and Bourell, 1996).

EOS GmbH (Munich, Germany) avoids the use of a polymer binder by directly sintering metal powders with a low melting point, i.e. bronze-nickel based powders (EOS-Cu 3201 containing Cu-Sn, Cu-P and Ni particles) developed by Electrolux Co. (Behrendt and Shellabear, 1995). An example is given in Figure 3(b). After SLS, the part is infiltrated with epoxy resin to fill in the porosities. Hence the final part is a bronze-epoxy composite, rather than a plain metallic part and its mechanical and thermal properties are limited (Table III). Infiltration with a metal like Cu or bronze is not possible in this case, since the green part would melt during infiltration. Recently, EOS put into market a new powder (EOS-DMLS Steel 50-V1 containing steel, Cu-P and Ni particles) yielding improved mechanical properties (PM update, 1998). The SLS part is about 70 per cent dense and thus can be used as such for inserts and small mould components.

2.3.2 SLS of metals and hardmetals/cermets by liquid phase sintering

Many research institutes study the possibility of directly laser sintering metal and ceramic powders without the use of any polymer component (Bourell *et al.*, 1992; Coremans *et al.*, 1996; Das *et al.*, 1996; Kruth *et al.*, 1996, 1997; Laoui *et al.*, 1998; O'Neill *et al.*, 1999; Song and Konig *et al.*, 1997; Van der Schueren and Kruth, 1994). For this purpose, several approaches for binding powder particles together using laser beam energy have been investigated at the University of Leuven including: solid state vs liquid phase sintering (LPS), loose vs pre-coated metal binder phase, mixed vs milled powders (Kruth *et al.*, 1996; Laoui *et al.*, 1998).

The basic material used in LPS consists of a mixture of two metal powders (or of a metal and a ceramic powder in case of hardmetals and cermets), i.e. a high melting point metal or ceramic, called the structural material, and a low melting point metal, called the binder. Applying heat to the system causes the binder to melt and flow into the pores formed by the non-molten particles. The classical stages of LPS are schematically shown in Figure 4.

Besides the very good mechanical properties generally obtained with two-phase

Figure 4 Different stages of LPS

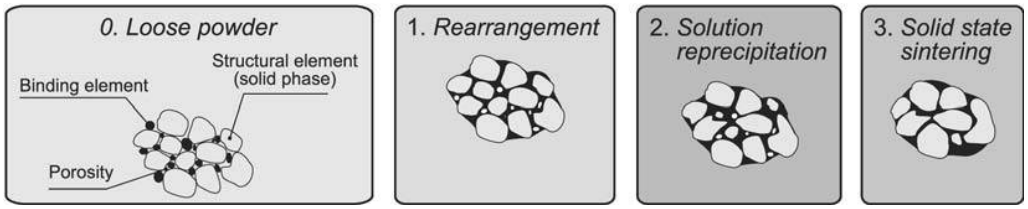

or composite LPS materials, the main advantage of LPS is the very fast initial binding occurring during laser heating. This binding is based on capillary forces, which can be very high: the reaction speed in this stage is determined by the kinetics of the solid-melt transformation. This transformation is several orders of magnitudes faster than solid-state diffusion of atoms occurring in the solid phase sintering.

Once the binder metal is molten and spread out into the solid lattice, the system cools down as the laser beam moves away and the situation is frozen. Only the first stage (rearrangement) of the LPS mechanism takes place during laser sintering because of the very short laser-material interaction time (fraction of a second).

Early studies to sinter steel or iron powder, mixed up with copper grains serving as binder material, were performed at several universities (Coremans *et al.*, 1996; Miani *et al.*, 2000; Song and Konig, 1997; Van der Schueren and Kruth, 1994). Figure 5 shows an example of a steel-copper powder mixture laser sintered at the University of Leuven. Such LPS green part has enough strength to withstand a post-processing cycle to bring the part to full density. This post-processing consists of a furnace post-sintering to proceed with the next stages of LPS shown schematically in Figure 4 (solution reprecipitation and solid state sintering) or an infiltration with a low melting point metal (typically copper or bronze).

The universities of Texas at Austin (USA) (Jepson *et al.*, 1999) and Leuven (Belgium) (Kruth *et al.*, 1997; Laoui *et al.*, 1998) and some German Fraunhofer research centres (Private communication, 1999) succeeded to laser sinter hardmetals (i.e. cemented carbides) and cermets by SLS. Figure 6(a) shows a typical microstructure of a WC-9 wt per cent Co powder mixture sintered by a CO_2 laser showing a good bounding between the WC particles surrounded by a Co-binder and the presence of large pores (50-60 per cent). After infiltration, Cu filled these open porosities (Figure 6(b)). Examples of WC-Co parts sintered at the University of Leuven are depicted in Figure 7.

A wide variety of powder combinations have been investigated in Leuven using LPS mechanism, including: Fe-Cu, Cu-coated Fe, Fe_3C-Fe, stainless steel-Cu, WC-Co, co-coated WC, WC-Cu, WC-CuFeCo, TiC-Ni/Co/Mo, TiB_2-Ni, ZrB_2-Cu, etc.(Laoui *et al.*, 1999b).

Significant improvements were obtained when using composite powders, obtained by mechanical alloying a mixture of two powder

Figure 5 SLS of steel-copper powder mixture

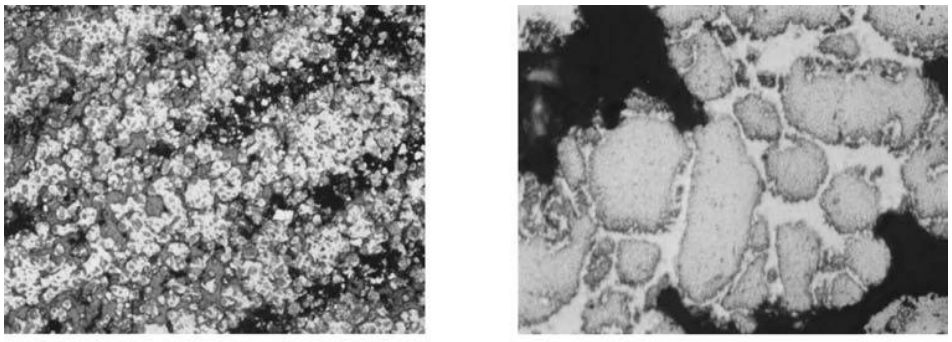

a) View of several laser sintering tracks

b) Detail showing non-molten steel particles bounded in molten Cu

Figure 6 SLS of WC-9 wt per cent Co powder mixture, followed by Cu infiltration

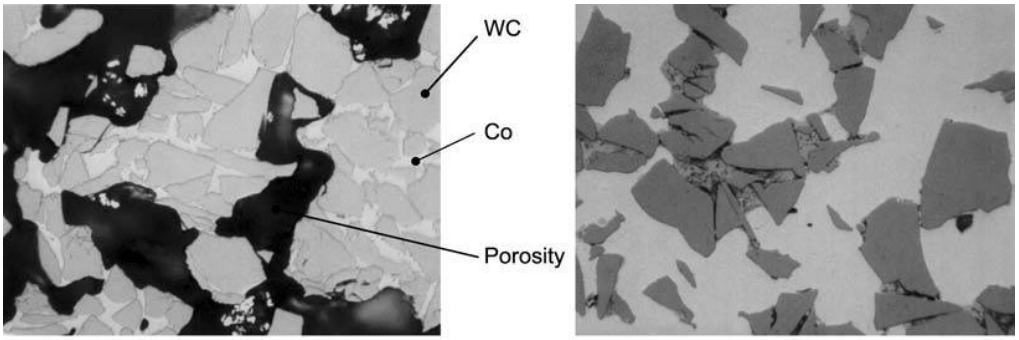

a) WC particles bound in Co matrix after SLS *b) Same after infiltration with Cu*

Figure 7 Various WC-Co parts made by SLS

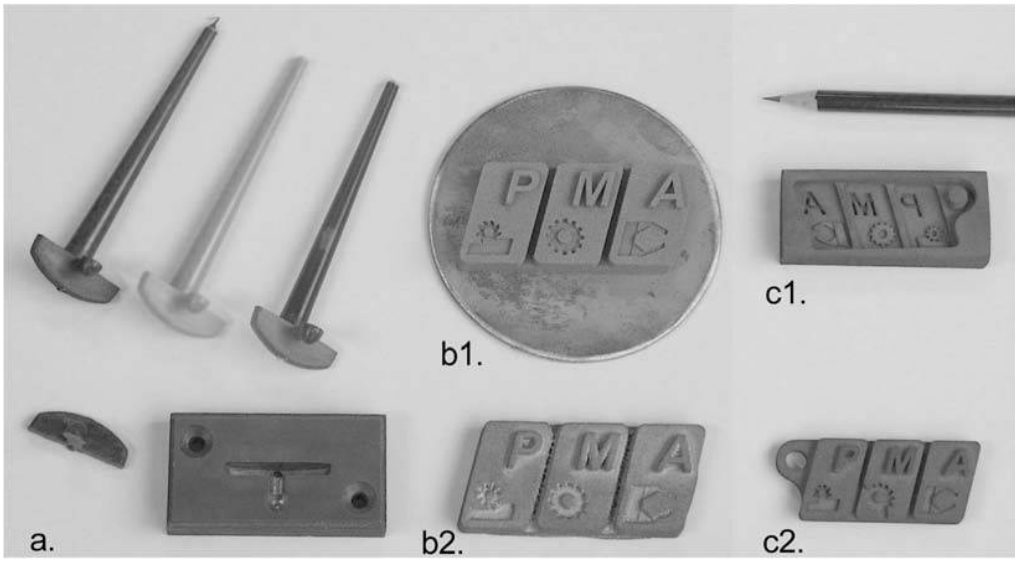

a. WC-Co mould insert infiltrated with Cu and injected plastic parts
b. PMA logo before (b1 = green part) and after (b2) Cu infiltration
c. PMA keyholder: Cu infiltrated mould insert (c1) and Cu infiltrated SLS part (c2)

materials (e.g. mixture of WC and Co powder particles as shown in Figure 8(a1). During mechanical alloying, the individual powder particles are milled, repeatedly fractured and welded together. This results in new powder particles depicting a fine micrograin composite structure in which two phases (i.e. the two original materials, here WC and Co) can still be identified (Figure 8(b1)). Laser sintering WC-9 wt per cent Co mechanically alloyed powder (Figure 8(b2)) resulted in higher green densities with better surface roughness as compared to direct laser sintering of a WC-9 wt per cent Co powder mixture not subjected to mechanical alloying (Figure 8(a2)) (Laoui *et al.*, 1999a).

2.3.3 SLS of metals through melting

The Fraunhofer Institute ILT (Aachen, Germany) applied a 300 W Nd:YAG laser to completely melt metal powders (bronze, steel, stainless steel such as 316L) deposited in a standard way using a wiper (scraper) and producing directly dense parts (density $>$ 95 per cent) (Klocke *et al.*, 1996). Due to the tendency of molten metal to form droplets and minimise surface energy, careful control of the process parameters is needed. Moreover, overhangs with angles higher than 60° could not be built with this process. When this process was used to sinter Al-30 per cent Si, a maximum density of 90-95 per cent was obtained (Private communication, 1999).

Figure 8 SLS of mixed (unalloyed) and milled (alloyed) WC-Co powder

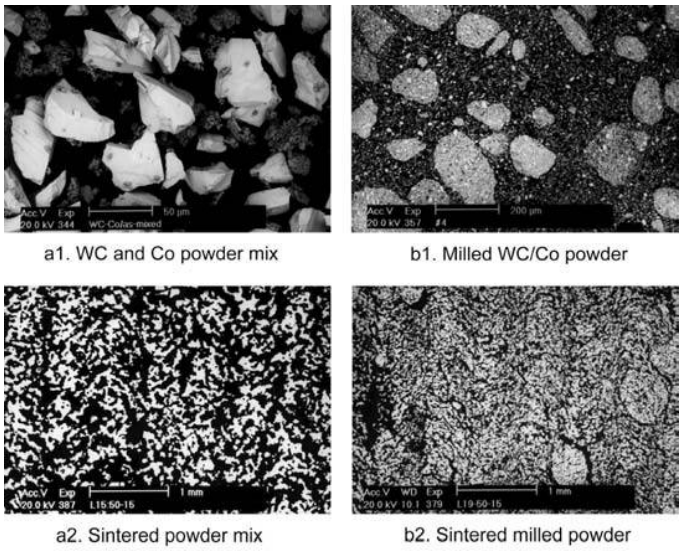

Note: White = WC; Grey = Co, Black = pores

EOS recently came to the market with a plain steel powder that is laser sintered through melting. The average particle size is 50 μm, but an enhanced steel powder with 20 μm size is announced.

Osaka University (Japan) utilised a pulsed Nd:YAG laser (50 W mean power, 3 kW maximum peak power) to melt pure Ti spherical powders (200 and 50 μm average particle size) to produce medical parts (dental crowns and bone models) (Abe *et al.*, 2000). For the coarse Ti powder, the SLS part delivered a maximum relative density of 84 per cent yielding a maximum tensile strength of 70 MPa. Using fine Ti powder (25 μm), a higher relative density (maximum 93 per cent) was achieved with a tensile strength of 150 MPa. Due to the presence of remaining porosity, the tensile strength of these SLS parts is still lower than that of bulk pure Ti material (275-481 MPa) (Abe *et al.*, 2000).

2.4 SLS of ceramics

The Fraunhofer Institute IPT used the SLS process in an attempt to produce directly ceramic parts without polymer binder material. The absence of any binder element makes the ceramic laser sintered part very fragile and viable to breakage. Due to the short reaction time involved in SLS, solid state sintering is not feasible. To sinter SiC powder material, a sufficient amount of laser energy was supplied to induce high local temperatures leading to a partial disintegration of SiC particles into Si and C. The free Si then oxidises and forms SiO_2, which plays a role of a binder between the SiC particles (Klocke and Wirtz, 1997; Klocke *et al.*, 1996). After laser sintering, the SiC parts could be infiltrated with Si and reaction bonded to full density. Zirconium silicates were also laser sintered by almost fully melting the powder particles forming large agglomerates (Klocke and Wirtz, 1997, 1998). Similar to DTM's polymer coated powder process, graphite coated with phenolic resin was also processed by SLS by melting only the polymer binder, which is burned out afterwards. However, the resulting graphite part becomes very fragile (Klocke and Wirtz, 1997).

2.5 SLS of foundry sand

The two commercial SLS machine vendors (DTM and EOS) offer sand powders that can be laser sintered in order to produce foundry sand moulds. DTM, for instance, offers both Zr and Si sand: SandForm ZrII and Si (Seitz, 1998). Key characteristics include Shell Foundry Sand of given AFS grain fineness number (GFN# = 97 for Si and 99 for ZrII) and dimensional tolerances of 0.5 mm. SandForm Si, used predominantly for Al castings, is based on silica, which is prevalent in the market and has a low density. SandForm ZrII can be used for both Al and Fe castings and its binder system matches silica.

3. Lasers and materials

Different kind of lasers are applied in SLS. Commercial SLS machines (DTM and EOS) are all equipped with CO_2 lasers with maximum power ratings between 50 and 200 W. The University of Leuven developed two SLS machines equipped, respectively, with continuous wave Nd:YAG lasers of 300 and 500 W (Van der Schueren and Kruth, 1995a). So did others (Klocke and Wirtz, 1996; Laoui *et al.*, 1999b; Song and Konig, 1997). The University of Liverpool explored the use of Q-switched Nd:YAG and short-pulse Cu-vapour lasers (O'Neill *et al.*, 1999). The University of Connecticut and University of Manchester used a 60 W diode laser of 810 nm (Li *et al.*, 1998; Manzur *et al.*, 1996). In future, other type of lasers might

show up like diode pumped solid-state lasers and others.

The choice of a proper SLS laser might not be independent of the material to be sintered. Varying SLS process parameters like laser wavelength (i.e. type of laser), laser energy (i.e. power, scan speed and scan spacing) and powder characteristics (particle size, powder composition, mixing, etc.), greatly influences the resulting part properties such as surface quality or part density (Laoui *et al.*, 1998, 1999a). Optimally, the laser wavelength should be adapted to the powder material to be sintered, since laser absorption greatly changes with the material and frequency or wavelength of the laser light (Olsen and Femming, 1989; Tolochko *et al.*, 2000). Figure 9 shows how absorption coefficients varies versus wavelength for a solid polymer (PC) and metal (Cu). Laser absorption in powders is usually larger than in solid material. This is due to multiple reflection and absorption of the laser beam trapped in the pores of the powder (Figure 12). In order to distinguish between the basic material absorption coefficient of solid material upon a single impingement of a laser ray and the total absorption of a powder upon multiple impingement (i.e. multiple partial absorption and partial reflection), let us call the former as "material absorption" and the later as "powder incoupling". Results of measurements of laser incoupling in powders performed with an integrating sphere are reported in Table IV (Tolochko *et al.*, 2000). Measurements with single component powders (Ni-alloy) of different particle sizes proved that the particle size has little influence on the incoupling. This statement is confirmed by simulations (see further), but is no longer true when mixing two powders of different material and different grain size (see simulation results below).

CO_2 lasers with wavelength of 10.6 μm are well suited for sintering polymer powders, as polymers depict high absorption at far infrared or long wavelength (see Table IV and Figure 9). The same is true for oxide ceramics, but no longer for carbide ceramics that better absorb at Nd:YAG wavelength of 1.06 μm (Table IV). It is also well known that metals absorb much better at short wavelength (Table IV and Figure 9). This is why Nd:YAG lasers may outperform CO_2 lasers for metallic materials. The latter is particularly true for LPS of metallic materials and has been confirmed by studies of the University of Leuven in which Fe-Cu metal powders and WC-Co hardmetal or cermet powders were alternatively sintered with both laser types (Kruth *et al.*, 1998b). Experiments proved that for the same amount of energy (or at similar settings for laser power and scan speed), a Nd:YAG laser results in higher green part density (Figure 10), a larger sintering depth (allowing thicker layers to be sintered, hence reducing production time) and a higher energetic process efficiency. Figure 11 also shows that, for those materials, the processing window where a YAG laser yields proper LPS is larger than that of a CO_2 laser, as well as in terms of allowable range of supplied energy as of powder composition. This allows a wide variation of the processing parameters (power and scan speed) or powder composition (here mixture ratio between Fe and Cu), while still ensuring good sintering results (i.e. proper LPS, yielding fine composite structure and better part properties as compared to true melting). The large processing window enforces good process controllability and reliability.

The small LPS processing window in the case of CO_2 is explained by the small difference in melting points between the structural element (stainless steel) and the binder element (Cu) and by the high reflectivity of Cu particles for CO_2 laser light. This induced mostly simultaneous melting of both elements, rather than preferential melting of the Cu binder and resulted in reduced mechanical properties. Owing to the larger difference in their melting points, such behaviour was not observed with WC-Co

Figure 9 Absorption of plain solid materials (PC and copper) versus wavelength

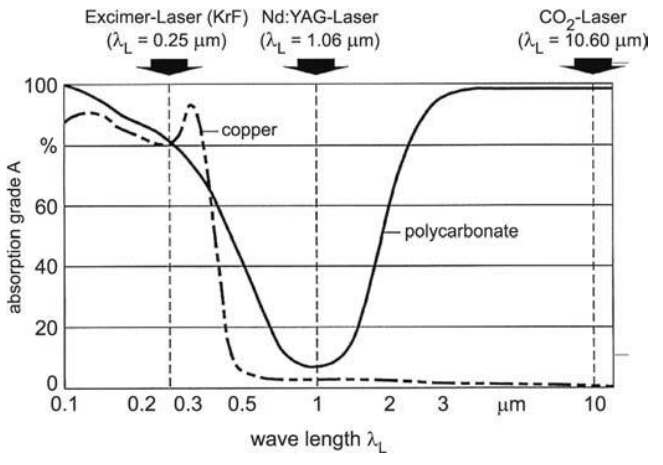

Table IV Incoupling (absorption) of powder materials for Nd:YAG and CO_2 wavelength

Powder materials	Nd:YAG (1.06 μm)	CO_2 (10.6 μm)
Metals		
Cu (absorption in solid Cu)	59 per cent (2-10 per cent*)	26 per cent (1 per cent)
Fe (absorption in solid Fe)	64 per cent (30 per cent)	45 per cent (4 per cent)
Sn	66 per cent	23 per cent
Ti	77 per cent	59 per cent
Pb	79 per cent	–
Co-alloy (1 per cent C; 28 per cent Cr; 4 per cent W)	58 per cent	25 per cent
Cu-alloy (10 per cent Al)	63 per cent	32 per cent
Ni-alloy 1 (13 per cent Cr; 3 per cent B; 4 per cent Si; 0.6 per cent C)	64 per cent	42 per cent
Ni-alloy 2 (15 per cent Cr; 3.1 per cent Si; 0.8 per cent C)	72 per cent	51 per cent
Ceramics		
ZnO	2 per cent	94 per cent
Al_2O_3	3 per cent	96 per cent
SiO_2	4 per cent	96 per cent
SnO	5 per cent	95 per cent
CuO	11 per cent	76 per cent
SiC	78 per cent	66 per cent
Cr_3C_2	81 per cent	70 per cent
TiC	82 per cent	46 per cent
WC	82 per cent	48 per cent
Polymers		
Polytetrafluoroethylene	5 per cent	73 per cent
Polymethylacrylate	6 per cent	75 per cent
Epoxypolyether-based polymer	9 per cent	94 per cent
Mixtures		
Fe-alloys (3 per cent C; 3 per cent Cr; 12 per cent V) + 10 per cent TiC	65 per cent	39 per cent
Fe-alloys (1 per cent C; 14 per cent Cr; 10 per cent Mn; 6 per cent Ti) + 66 per cent TiC	79 per cent	44 per cent
Ni-alloy 2 (95 per cent) + Epoxypolyether-based polymer (5 per cent)	68 per cent	54 per cent
Ni-alloy 2 (25 per cent) + Epoxypolyether-based polymer (75 per cent)	23 per cent	76 per cent

Note: *Value varying with gloss, surface roughness, surface oxidation, etc.
Source: Tolochko *et al.* (2000)

powder mixtures where most of the SLS tests resulted in LPS without much difficulty. Further details about these results can be found elsewhere (Kruth *et al.*, 1998b; Laoui *et al.*, 1998, 2000a).

4. Modelling and simulation of material-laser behaviour

Several simulation models have been developed to get a better understanding of the SLS process and of the interaction between the laser beam and powder material. These models not only provide a theoretical explanation to the phenomena discussed above, but also have a major practical significance. Indeed, the final properties of parts fabricated by SLS very much depend on the process parameters as well as on the powder characteristics. Simulation allows to identify the processing window and to select proper SLS parameters without need for extensive testing for each powder.

Figure 10 Relative density of stainless steel-Cu SLS parts processed by CO_2 and Nd:YAG lasers

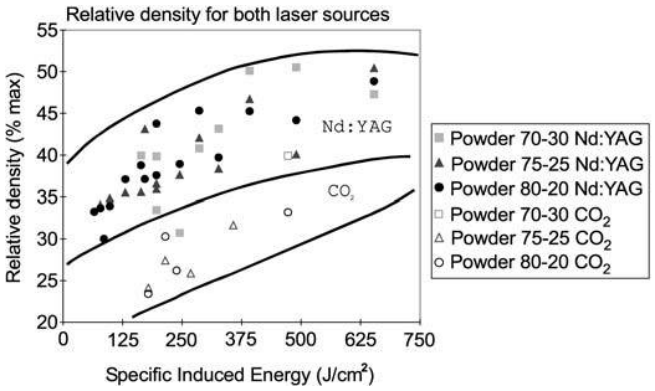

Many researchers apply thermal finite element methods to model the SLS process (Childs *et al.*, 1999, 2000; Nelson, 1993; Wang and Kruth, 2001; Weissman and Hsu, 1991). Those models need a heat source to be defined, which in turn requires to postulate the powder absorption (incoupling) and the depth at which the absorption takes places. FEM models also need to assume the heat conductivity in the powder, which is generally very low and even negligible (Wang and Kruth, 2001). In most FEM models, a surface heat source is assumed, neglecting the penetration of the laser beam into the powder bed (porosity). A volumetric heat source has been applied by Childs *et al.* (2000) and Wang and Kruth (2001), demonstrating that the depth of the heat source into the powder bed largely influences the quality of the simulation.

A ray tracing (RC) model has been developed at the University of Leuven (Laoui *et al.*, 2000b; Wang and Kruth, 2000). It is based on a geometrical simulation of the impingement, reflection and absorption of a large number of rays (representing the laser beam) onto/into a powder bed (Figure 12). Each time a ray hits a powder particle, the amount of absorbed and reflected energy is calculated and the reflected ray is traced further along its way into the pores of the powder bed. This model allows to calculate:

- the powder incoupling E (i.e. total absorption) versus the material absorption coefficient α: see Figure 13 (relation between incoupling and material absorption coefficient for single component powder) and Table V (total incoupling into Fe-Cu and WC-Co powder mixture for Nd:YAG and CO_2 laser);
- the amount of energy absorbed by each powder material in the case of powder mixtures Table V;
- the laser beam penetration and the absorption profile versus the depth into the powder bed (Figure 14);
- the sintering depth and width of a single laser track (Figure 15).

The RC simulations demonstrate the following.

- Incoupling in powders is much higher than in solid material, mainly for materials with low absorption coefficients where the increase is more than an order of magnitude (see Figure 13 and experimental data on Cu in Table IV).
- The maximum of the absorption profile of a CO_2 laser lies deeper under the powder bed surface than for a Nd:YAG laser (Figure 14). However, the larger total incoupling with Nd:YAG laser (see Table V) still results in a larger sintering depth with that laser.
- In the case of powder mixtures, the relative particle size of the two powder components largely influences the relative amount of energy absorbed by each powder material. This is illustrated in

Figure 11 Processing window for stainless steel-Cu sintered by CO_2 and Nd:YAG laser

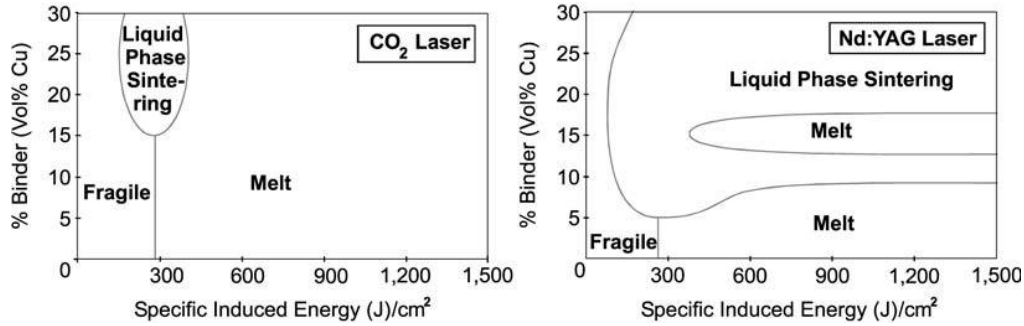

Figure 12 2D illustration of the RC model: simulation over a depth of 1 mm and width of 1 mm of powder bed

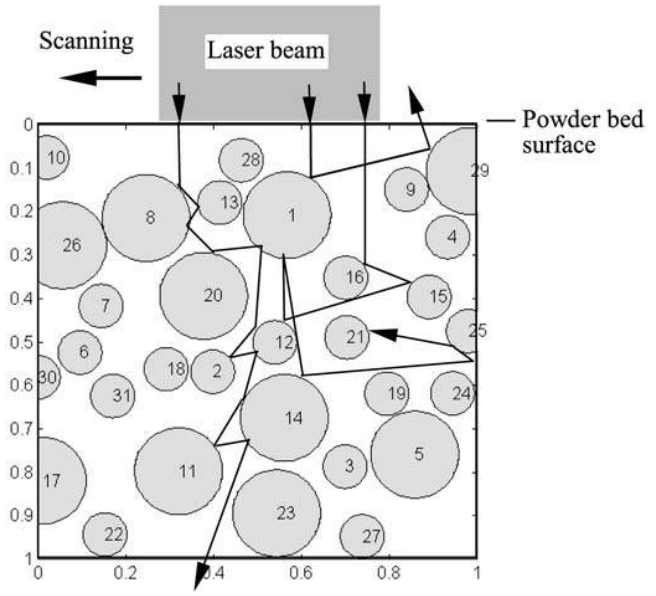

Table VI for a mixture of Fe and Cu particles regularly stacked according to a phase centred structure and sintered with a Nd:YAG laser (Van der Schueren and Kruth, 1994). When mixing Fe and Cu particles of equal size or diameter (Simulation 1), the less reflective Fe will absorb more energy and achieve its melting point before the high reflective Cu starts melting (comparing required and absorbed energies), even though Fe has a much higher melting point than Cu (1,500°C versus 1,083°C). To enforce proper LPS, where only the Cu melts and binds the solid Fe particles, the Cu particles should be taken smaller than the Fe particles (Simulations 2, 3 and 4).

- The RC model demonstrates a good accuracy when comparing the results to the experimental data (Figure 13, compare also to Cu and Fe values in Table IV). Comparison of sintering depth and width calculated solely with the RC model and those calculated with a combined RC-FEM model (RC model provides heat input profile for thermal FEM simulation) show little difference (Wang and Kruth, 2001) (Figure 15). This indicates that, in most cases, FEM simulations do not add much to the precision of the RC model. This is due to the almost negligible heat conductivity in porous powder beds.

As shown in Table VI, the RC model further allows to analyse the influence of various parameters like particle diameter, mixture ratio, type of material (i.e. material absorption coefficient), etc.

5. Conclusion

SLS holds an important place among the wide variety of rapid prototyping processes (Kruth, 1991; Kruth *et al.*, 1998a). One of its major advantages is the ability to process about any (powder) material: polymers (elastomers, amorphous and semi-crystalline technical polymers), metals, hardmetals/cermets,

Figure 13 Total energy incoupling versus the material absorption coefficient: modelling and experiments

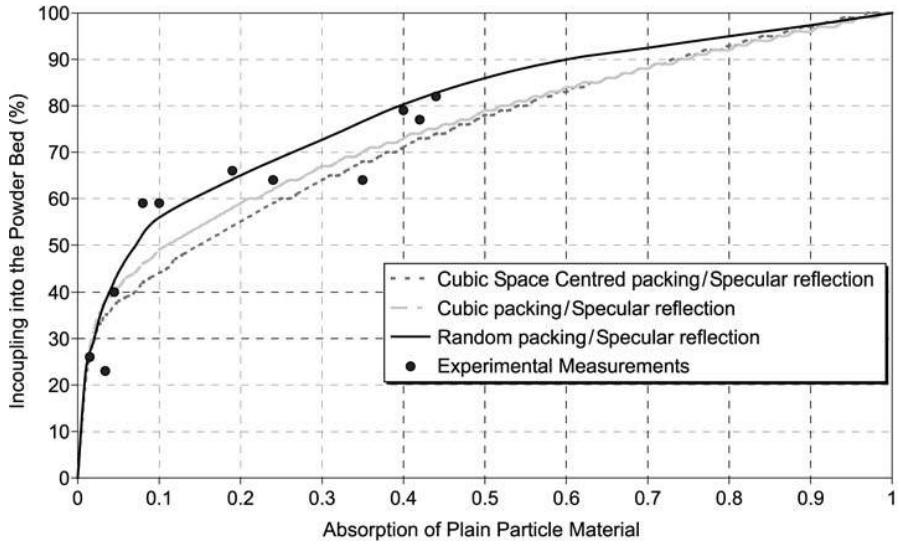

Table V Incoupling *E* (per cent) when sintering powder mixtures with porosity of about 75 per cent of full density

Powder (grain size)	Type of laser	$\lambda(\mu m)$	$\alpha_{Fe,\ resp.\ WC}$ (per cent)	$\alpha_{Cu,\ resp.\ Co}$ (per cent)	E_{total} (per cent)	E_{Fe} (per cent)	E_{Cu} (per cent)
Fe-30 wt per cent Cu (Fe = 50 μm; Cu = 30 μm)	Nd:YAG	1.06	30	10	66	54	12
	CO_2	10.6	3.5	1.5	26.5	21	6
WC-9 wt per cent Co (WC = 50 μm; Co = 20 μm)	Nd:YAG	1.06	55	31	80	61	19
	CO_2	10.6	??	2.6	–	–	–

Figure 14 Energy absorption profiles versus the depth into the powder bed

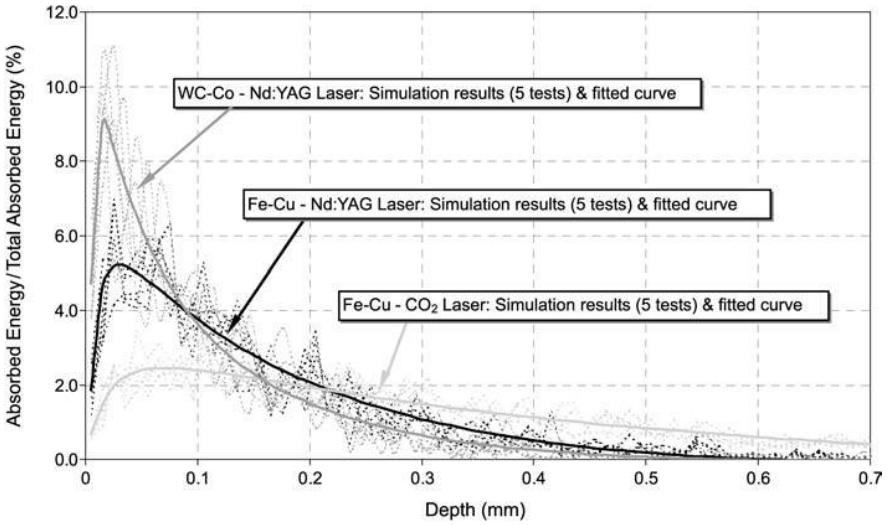

Figure 15 Track thickness and width when sintering Fe-Cu powder with Nd:YAG laser

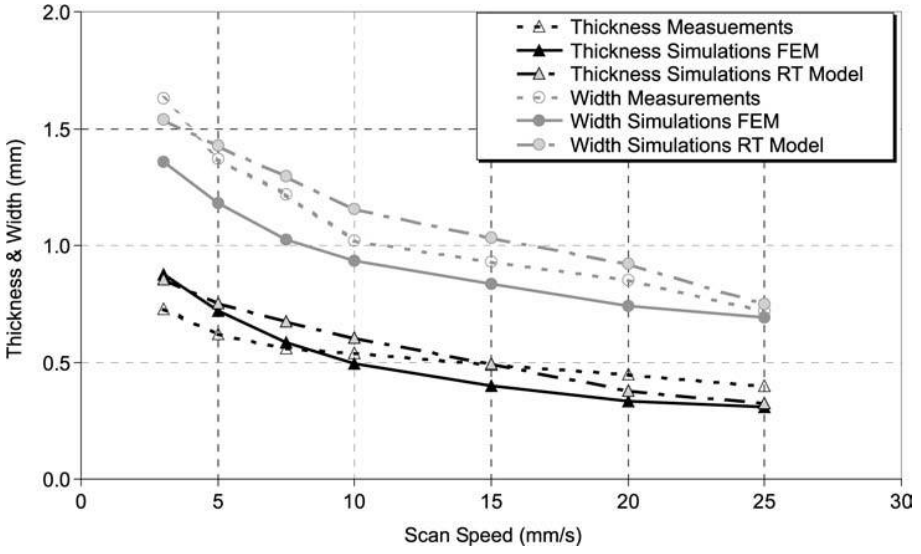

ceramics and sand. Among others, SLS is well suited to produce a variety of composite materials: glass reinforced polymers, metal/polymer composite (e.g. Cu/PA), metal/metal composites (e.g. Fe/Cu), cermets (e.g. WC-Co) and others. In many cases, standard off-the-shelf powder materials can be used, without the need to develop dedicated powders. Quite some developments, however, aim to develop powders specially tuned for selecting laser sintering. The purpose is to have powders depicting finer particle size (thinner layers, better resolution and finer roughness), better flowability (for easier powder layer deposition); less shrinkage during laser

Table VI Simulation results for mixtures Fe and Cu powder particles regular stacked as successive layers of grains (phase centred packing). A single sintered powder layer contains several layers of grains

	Simulation parameters				Simulation results	
	Parameter	Fe	Cu	Energy mJ (per cent)	Fe	Cu
1	**Diameter (μm)**	**50**	**50**	Required for melting	**0.45**	0.32
	Absorptivity (per cent)	30	10	Absorbed by layer 1	**0.45** (25.3 per cent)	0.037 (2.1 per cent)
	Mixture ratio (per cent)	80	20	Absorbed by layer 2	0.38 (21.4 per cent)	0.032 (1.8 per cent)
2	**Diameter (μm)**	**50**	**10**	Required for melting	0.45	**0.0026**
	Absorptivity (per cent)	30	10	Absorbed by layer 1	0.031 (25.3 per cent)	**0.0026** (2.1 per cent)
	Mixture ratio (per cent)	80	20	Absorbed by layer 2	0.026 (21.4 per cent)	0.0022 (1.8 per cent)
3	**Diameter (μm)**	**50**	**30**	Required for melting	0.45	**0.069**
	Absorptivity (per cent)	30	10	Absorbed by layer 1	0.31 (20 per cent)	**0.069** (4.4 per cent)
	Mixture ratio (per cent)	**60**	**40**	Absorbed by layer 2	0.26 (16.5 per cent)	0.058 (3.7 per cent)
4	**Diameter (μm)**	**50**	**30**	Required for melting	0.45	**0.069**
	Absorptivity (per cent)	30	**20**	Absorbed by layer 1	0.41 (24.5 per cent)	**0.069** (4.1 per cent)
	Mixture ratio (per cent)	80	20	Absorbed by layer 2	0.32 (19.4 per cent)	0.054 (3.2 per cent)

Source: Van der Schueren and Kruth (1994)

sintering (no part warpage), higher green density, higher strength, etc.

The quality of laser sintered parts, however, greatly depends on proper selection of the processing parameters. The latter not only comprises the adjustable machine parameters (like laser power, spot size, scanning speed, etc.), but also the type of laser (wavelength) and the powder composition (materials, mixture ratios, grain sizes, etc.). This is because the SLS process is not only controlled by the amount and speed of energy supply, but to a great extent by the basic laser-material interaction. Experimental research is going on to better understand this interaction. Simulation models proved beneficial for demonstrating the influence of the various parameters. Those models are the essential tools for identifying proper parameters without extensive testing.

References

Abe, F. *et al.* (2000), "Manufacturing of Ti parts for medical purposes by selective laser melting", *Proc. 8th Int. Conf. on Rapid Prototyping*, pp. 288-93.

Behrendt, U. and Shellabear, M. (1995), "The EOS rapid prototyping concept", *Computers in Industry*, Vol. 28, pp. 57-61.

Bourell, D.L., Marcus, H.L. and Beaman, J.J. (1992), "Selective laser sintering of metal and ceramics", *Int. J. Powder Metallurgy*, Vol. 28 No. 4, pp. 369-81.

Bruning, S. (1998), "Copper polyamide", *2nd Europ. SLS users meeting*, K.U. Leuven, Belgium, pp. 1-10.

Childs, T.H.C., Berzins, M., Ryder, G.R. and Tontwi, A.E. (1999), "Selective laser sintering of an amorphous polymer – simulations and experiments", *Proc. I. Mech. E., Part B, J. of Eng. Manufacture*, Vol. 213, pp. 333-49.

Childs, T.H.C., Hauser, C., Taylor, C.M. and Tontwi, A.E. (2000), "Simulation and experimental verification of crystalline polymer and direct metal selective laser sintering", *Proc. 11th Annual Solid Freeform Fabrication Symposium*, 7-9 August, University of Texas, Austin, USA (in press).

Coremans, A., Kauf, M. and Hoffman, P. (1996), "Laser assisted rapid tooling of molds and dies", *Proc. 5th Europ. Conf. on Rapid Prototyping and Manuf.*, pp. 195-210.

Das, S., Beaman, J.J., Wohlert, M. and Bourell, D. (1998), "Direct laser freeform fabrication of high performance metal components", *Proc. 7th Europ. Conf. on RP&M*, Aachen, Germany, pp. 297-306.

Das, S., Harlan, N., Beaman, J.J. and Bourell, D.L. (1996), "Selective laser sintering of high performance high temperature metals", *Proc. Solid Freeform Fabrication Symposium*, pp. 89-95.

Dormal, Th., Dam, J.L. and Baraldi, U. (1998), "A new technology for the manufacturing of large prototype injection moulds, laminated laser cut cavities (LLCC)", *Proc. 7th Eur. Conf. on Rapid Prototyping and Manufacturing*, pp. 327-36.

Fessler, J., Nickel, G., Link, G., Prinz, F. and Fussel, P. (1998), "Functional gradients in metallic prototypes", *Prototyping Technology Int. '98*, UK and International Press, Dorking, UK, pp. 160-3.

Griffith, M.L., Keichder, D.M. and Atwood, C.L. *et al.* (1996), "Free fabrication of metallic components using laser engineered net shaping (LENS)", *Solid Freeform Fabrication Conf. Proc.*, Austin, TX, pp. 125-31.

Grimm, R. (1997), "SLS and SLA, different technologies for different applications", *Prototyping Technology International '97*, UK and Intern. Press, Dorking, UK, pp. 130-8.

Heymadi, U. and McAlea, K. (1996), "Selective laser sintering of metal molds, the rapid tool process", *Solid Freeform Fabrication Proceedings*, pp. 97-104.

Himmer, T., Nakagawa, T. and Anzai, M. (1999), "Lamination of steel sheets", *Computers in Industry*, Vol. 39 No. 1, pp. 27-34.

Jepson, L., Perez, J., Beaman, J.J., Bourell, D. and Wood, K. (1999), "Initial development of a multi-material selective laser sintering process (M^2SLS)", *Proc. 8th Europ. Conf. on RP&M*, pp. 367-84.

Klocke, F. and Clemens, U. (1996), "Rapid tooling combining laser generating and high speed milling", *Proc. 5th Europ. Conf. on Rapid Prototyping and Mfg.*, pp. 211-21.

Klocke, F. and Wirtz, H. (1997), "Selective laser sintering of ceramics", *Proc. LANE'97 Conf., Laser Assisted Net Shape Eng.*, Vol. 2, pp. 589-96.

Klocke, F. and Wirtz, H. (1998), "Selective laser sintering of zirconium silicate", *Proc. 7th European Conf. on Rapid Prototyping and Manufacturing*, Aachen, Germany, pp. 307-14.

Klocke, F., Wirtz, H. and Meiners, W. (1996), "Direct manufacturing of metal prototypes and prototype tools", *Proc. Solid Freeform Fabrication Symposium*, pp. 141-8.

Knight, R., Knight, J., Beaman, J.J. and Freitag, D. (1996), "Metal processing using selective laser sintering and hot isostatic pressing (SLS/HIP)", *Proc. SFF Symposium*, Austin, pp. 349-53.

Kruth, J-P. (1991), "Material incress manufacturing by rapid prototyping techniques", *Annals of the CIRP*, Vol. 40 No. 2, pp. 603-14 (Keynote paper).

Kruth, J-P., Leu, M.C. and Nakagawa, T. (1998a), "Progress in additive manufacturing and rapid prototyping", *Annals of the CIRP*, Vol. 47 No. 2, pp. 525-40 (Keynote paper).

Kruth, J-P., Froyen, L., Morren, B. and Bonse, J.E. (1997), "Selective laser sintering of WC-Co 'hard metal' parts", *Proc. 8th Int. Conf. on Production Engineering (ICPE-8), Rapid Product Development*, ISBN 0-412-81160X, Chapman and Hall, London, pp. 149-56.

Kruth, J-P., Peeters, P., Smolderen, T., Bonse, J., Laoui, T. and Froyen, L. (1998b), "Comparison of CO_2 and Nd-YAG lasers for use with selective laser sintering of steel-copper powders", *Int. Journal of CADCAM and Computer Graphics*, Vol. 13 Nos 4-6, pp. 95-110.

Kruth, J-P. *et al.* (1996), "Basic powder metallurgical aspects in selective metal powder sintering", *Annals of the CIRP*, Vol. 45 No. 1, pp. 183-6.

Laoui, T., Froyen, L. and Kruth, J-P. (1999a), "Effect of mechanical alloying on selective laser sintering of WC-9Co powder", *Powder Metallurgy*, Vol. 42 No. 3, pp. 203-5.

Laoui, T., Froyen, L. and Kruth, J-P. (1999b), "Alternative binders to Co for WC particles for SLS process", *Proc. 8th Europ. Conf. on Rapid Prototyping and Manufacturing*, pp. 299-311.

Laoui, T., Bonse, J., Froyen, L. and Kruth, J-P. (1998), "Influence of powder parameters on selective laser sintering of tungsten carbide-cobalt", *Proc. 7th Europ. Conf. on Rapid Prototyping and Manufacturing*, pp. 271-9.

Laoui, T., Hespel, P., Kruth, J-P. and Froyen, L. (2000a), "Process optimization of WC-9Co parts made by selective laser sintering", *Proc. 8th Int. Conf. on Rapid Prototyping*, Tokyo, Japan, pp. 419-24.

Laoui, T., Wang, X., Childs, T.H.C., Kruth, J-P. and Froyen, L. (2000b), "Laser penetration in a powder bed during selective laser sintering of metal powders, simulations versus experiments", *Proc. 11th Annual Solid Freeform Fabrication Symp.*, 7-9 August, 2000, Univ. of Texas, Austin, USA, p. 1 (in press).

Li, L., Ng, K.L. and Slocombe, A. (1998), "Diode laser sintering of compacted metallic powders for desk top rapid prototyping", *Proc. 7th Europ. Conf. on Rapid Prototyping and Manuf.*, pp. 281-96.

Manzur, T., Roychoudhuri, C. and Marcus, H. (1996), "SFF using diode lasers", *Proc. Solid Freeform Fabrication Symposium*, pp. 363-8.

McAlea, K. (2000), "DTM's selective laser sintering technology, new products, new benefits, new manufacturing horizons", *Proc. 8th Int. Conf. on Rapid Prototyping*, + Conf. Presentation, pp. 347-52.

McAlea, K. *et al.* (1997), "Materials and applications for the selective laser sintering process", *Proc. 7th Int. Conf. on Rapid Prototyping*, pp. 23-33.

Miani, F. *et al.* (2000), "New iron based experimental powders for the direct metal selective laser sintering", *Proc. 9th Europ. Conf. on RP&M*, Athens, pp. 265-74.

Nelson, C. (1993), *Doctoral Dissertation*, The University of Texas at Austin.

O'Neill, W., Sutcliffe, C.J., Morgan, R., Landsborough, A. and Hon, K.K.B. (1999), "Investigation on multi-layer direct metal laser sintering of 316L stainless steel powder beds", *Annals of the CIRP*, Vol. 48 No. 1, pp. 151-4.

Olsen, F. and Femming, O. (1989), "Theoretical investigations in the fundamental mechanisms of high intensity laser light reflectivity", in Quenzer, A. (Ed.), High Power CO_2 Laser Systems and Applications, *Proc. of SPIE*, Vol. 1020, pp. 114-22.

P.M. update (1998), "EOS expands its range of metal powders for rapid prototyping users", *Metal Powder Report*, p. 6.

Private communication (1999), From Fraunhofer Institute IWS (Dresden, Germany) and Fraunhofer Institute ILT (Aachen, Germany).

Schumacher, B.M. and Levy, G.N. (1998), "Selective laser sintering combined with systematic development of new powders enabling innovative and prosperous redesign of process-layouts", *Proc. 12th Int. Symp. for Electro-Machining*, pp. 633-9.

Seitz, S. (1998), "Investment casting", *2nd Europ. SLS users meeting*, K.U. Leuven, Belgium, pp. 1-17.

Seitz, S. *et al.* (1997), "New materials for new applications in SLS", *Proc. LANE'97*, pp. 623-8.

Song, Y. and Konig, W. (1997), "Experimental study of the basic process mechanism for direct selective laser sintering of low-melting metallic powder", *Annals of the CIRP*, Vol. 46 No. 1, pp. 127-30.

Tolochko, N.K., Laoui, T., Khloplov, Y.V., Mozzharov, S.E., Titov, V.I. and Ignatiev, M.B. (2000), "Absorptance of powder materials suitable for laser sintering", *Rapid Prototyping Journal*, Vol. 6 No. 3, pp. 155-60.

Van der Schueren, B. and Kruth, J-P. (1994), "Laser based selective metal powder sintering, a feasibility study", *Proc 26th Int. CIRP Sem. on Manufacturing Systems, LANE'94*, pp. 793-802.

Van der Schueren, B. and Kruth, J-P. (1995a), "Design aspects of a 'selective metal powder sintering'

apparatus", *Proc. 11th Int. Symp. for Electro-Machining (ISEM-XI)*, pp. 651-62.

Van der Schueren, B. and Kruth, J-P. (1995b), "Powder deposition in selective metal powder sintering", *Rapid Prototyping Journal*, Vol. I No. 3, pp. 23-31.

Wang, X. and Kruth, J-P. (2000), "A simulation model for direct selective laser sintering of metal powders", *Computational Techniques for Materials, Composites and Composite Structures*, Civil-Comp Press, Edinburg, pp. 57-71.

Wang, X. and Kruth, J-P. (2001), "Finite element analysis of thermal process in selective laser sintering", *1st Int. Seminar on Progress in Innovative Manufacturing Engineering*, 20-22 June 2001, Genoa, Italy.

Weissman, M. and Hsu, M.B. (1991), "A finite element model of multi-layer sintered parts", *Proc. 2nd Solid Freeform Fabrication Symposium*, University of Texas, Austin, USA, pp. 86-94.

Wohlert, M. and Bourell, D. (1996), "Rapid prototyping of Mg/SiC composites by a combined SLS and pressureless infiltration process", *Proc. Solid Freeform Fabrication Symposium*, pp. 79-87.

Further reading

Wang, X. *et al.* (2001), "Direct selective laser sintering of hard metal powders, experimental study and simulation", *J. Adv. Manuf. Techn.*, (accepted for publication).

This article has been cited by:

1. Fuda Ning, Weilong Cong, Jingjing Qiu, Junhua Wei, Shiren Wang. 2015. Additive manufacturing of carbon fiber reinforced thermoplastic composites using fused deposition modeling. *Composites Part B: Engineering* **80**, 369-378. [CrossRef]
2. Fei Chang, Dongdong Gu, Donghua Dai, Pengpeng Yuan. 2015. Selective laser melting of in-situ Al4SiC4+SiC hybrid reinforced Al matrix composites: Influence of starting SiC particle size. *Surface and Coatings Technology* **272**, 15-24. [CrossRef]
3. Tatsuaki Furumoto, Ayato Koizumi, Mohd Rizal Alkahari, Rui Anayama, Akira Hosokawa, Ryutaro Tanaka, Takashi Ueda. 2015. Permeability and strength of a porous metal structure fabricated by additive manufacturing. *Journal of Materials Processing Technology* **219**, 10-16. [CrossRef]
4. Wei Zhu, Chunze Yan, Yunsong Shi, Shifeng Wen, Jie Liu, Yusheng Shi. 2015. Investigation into mechanical and microstructural properties of polypropylene manufactured by selective laser sintering in comparison with injection molding counterparts. *Materials & Design* . [CrossRef]
5. Min Seop Song, Hae Yoon Choi, Jee Hyun Seong, Eung Soo Kim. 2015. Matching-index-of-refraction of transparent 3D printing models for flow visualization. *Nuclear Engineering and Design* **284**, 185-191. [CrossRef]
6. Seung Kwon Seol, Daeho Kim, Sanghyeon Lee, Jung Hyun Kim, Won Suk Chang, Ji Tae Kim. 2015. Electrodeposition-based 3D Printing of Metallic Microarchitectures with Controlled Internal Structures. *Small* n/a-n/a. [CrossRef]
7. Benjamin Munro, Sid Becker, Marc Florian Uth, Niklas Preußer, Heinz Herwig. 2015. Fabrication and Characterization of Deformable Porous Matrices with Controlled Pore Characteristics. *Transport in Porous Media* **107**, 79-94. [CrossRef]
8. K. Bassett, R. Carriveau, S.-K.D. Ting. 2015. 3D printed wind turbines part 1: Design considerations and rapid manufacture potential. *Sustainable Energy Technologies and Assessments* . [CrossRef]
9. Pengpeng Yuan, Dongdong Gu. 2015. Molten pool behaviour and its physical mechanism during selective laser melting of TiC/AlSi10Mg nanocomposites: simulation and experiments. *Journal of Physics D: Applied Physics* **48**, 035303. [CrossRef]
10. Jason B. Jones, David I. Wimpenny, Greg J Gibbons. 2015. Additive manufacturing under pressure. *Rapid Prototyping Journal* **21**:1, 89-97. [Abstract] [Full Text] [PDF]
11. Raymond C. RumpfEngineering the Dispersion and Anisotropy of Periodic Electromagnetic Structures . [CrossRef]
12. Mingming Ma, Zemin Wang, Ming Gao, Xiaoyan Zeng. 2015. Layer thickness dependence of performance in high-power selective laser melting of 1Cr18Ni9Ti stainless steel. *Journal of Materials Processing Technology* **215**, 142-150. [CrossRef]
13. Qiong Nian, Martin Y. Zhang, Dong Lin, Suprem Das, Yung C. Shin, Gary J. Cheng. 2015. Crystalline photoactive copper indium diselenide thin films by pulsed laser crystallization of nanoparticle-inks at ambient conditions. *RSC Adv.* **5**, 57550-57558. [CrossRef]
14. Jonas Braier, Katharina Lattenkamp, Benjamin Räthel, Sandra Schering, Michael Wojatzki, Benjamin Weyers. 2014. Haptic 3D Surface Representation of Table-Based Data for People With Visual Impairments. *ACM Transactions on Accessible Computing* **6**:10.1145/2700996, 1-35. [CrossRef]
15. Boonlom Thavornyutikarn, Nattapon Chantarapanich, Kriskrai Sitthiseripratip, George A. Thouas, Qizhi Chen. 2014. Bone tissue engineering scaffolding: computer-aided scaffolding techniques. *Progress in Biomaterials* **3**, 61-102. [CrossRef]
16. Lei Wang, Jing Liu. 2014. Liquid phase 3D printing for quickly manufacturing conductive metal objects with low melting point alloy ink. *Science China Technological Sciences* **57**, 1721-1728. [CrossRef]
17. S.F. Wen, C.Z. Yan, Q.S. Wei, L.C. Zhang, X. Zhao, W. Zhu, Y.S. Shi. 2014. Investigation and development of large-scale equipment and high performance materials for powder bed laser fusion additive manufacturing. *Virtual and Physical Prototyping* 1-11. [CrossRef]
18. Jussi Putaala, Maciej Sobocinski, Saara Ruotsalainen, Jari Juuti, Petri Laakso, Heli Jantunen. 2014. Characterization of laser-sintered thick-film paste on polycarbonate substrates. *Optics and Lasers in Engineering* **56**, 19-27. [CrossRef]
19. Bethany C. Gross, Jayda L. Erkal, Sarah Y. Lockwood, Chengpeng Chen, Dana M. Spence. 2014. Evaluation of 3D Printing and Its Potential Impact on Biotechnology and the Chemical Sciences. *Analytical Chemistry* **86**, 3240-3253. [CrossRef]
20. P. Krakhmalev, I. Yadroitsev. 2014. Microstructure and properties of intermetallic composite coatings fabricated by selective laser melting of Ti–SiC powder mixtures. *Intermetallics* **46**, 147-155. [CrossRef]
21. Shwe P. Soe, Daniel R. Eyers. 2014. FEA support structure generation for the additive manufacture of CastForm™ polystyrene patterns. *Polymer Testing* **33**, 187-197. [CrossRef]
22. Fred L. Amorim, Armin Lohrengel, Volkmar Neubert, Camila F. Higa, Tiago Czelusniak. 2014. Selective laser sintering of Mo-CuNi composite to be used as EDM electrode. *Rapid Prototyping Journal* **20**:1, 59-68. [Abstract] [Full Text] [PDF]
23. Mohd Rizal ALKAHARI, Tatsuaki FURUMOTO, Takashi UEDA, Akira HOSOKAWA. 2014. Consolidation characteristics of ferrous-based metal powder in additive manufacturing. *Journal of Advanced Mechanical Design, Systems, and Manufacturing* **8**, JAMDSM0009-JAMDSM0009. [CrossRef]
24. Bin Qian, Zhijian Shen. 2013. Laser sintering of ceramics. *Journal of Asian Ceramic Societies* **1**, 315-321. [CrossRef]

25. B. Van Der Smissen, T. Claessens, P. Verdonck, P. Van Ransbeeck, P. Segers. 2013. Modelling the left ventricle using rapid prototyping techniques. *IRBM* **34**, 226-234. [CrossRef]
26. Fangxia Xie, Xinbo He, Xin Lu, Shunli Cao, Xuanhui Qu. 2013. Preparation and properties of porous Ti–10Mo alloy by selective laser sintering. *Materials Science and Engineering: C* **33**, 1085-1090. [CrossRef]
27. T.A. Krol, C. Seidel, M.F. Zaeh. 2013. Prioritization of Process Parameters for an Efficient Optimisation of Additive Manufacturing by Means of a Finite Element Method. *Procedia CIRP* **12**, 169-174. [CrossRef]
28. Andreas C. Fischer, Lyubov M. Belova, Yuri G. M. Rikers, B. Gunnar Malm, Henry H. Radamson, Mohammadreza Kolahdouz, Kristinn B. Gylfason, Göran Stemme, Frank Niklaus. 2012. 3D Free-Form Patterning of Silicon by Ion Implantation, Silicon Deposition, and Selective Silicon Etching. *Advanced Functional Materials* **22**:10.1002/adfm.v22.19, 4004-4008. [CrossRef]
29. Tatsuaki Furumoto, Takashi Ueda, Toru Amino, Daiki Kusunoki, Akira Hosokawa, Ryutaro Tanaka. 2012. Finishing performance of cooling channel with face protuberance inside the molding die. *Journal of Materials Processing Technology* **212**, 2154-2160. [CrossRef]
30. Krishna C.R. Kolan, Ming C. Leu, Gregory E. Hilmas, Mariano Velez. 2012. Effect of material, process parameters, and simulated body fluids on mechanical properties of 13-93 bioactive glass porous constructs made by selective laser sintering. *Journal of the Mechanical Behavior of Biomedical Materials* **13**, 14-24. [CrossRef]
31. Maurizio Fenech, Maurice Grech, John C. Betts. 2012. The in-flight temperature variation and dissolution of WC powder particles producing an Fe–Cr–W–C system by direct laser deposition. *Surface and Coatings Technology* **207**, 211-217. [CrossRef]
32. Jordi Delgado, Joaquim Ciurana, Ciro A. Rodríguez. 2012. Influence of process parameters on part quality and mechanical properties for DMLS and SLM with iron-based materials. *The International Journal of Advanced Manufacturing Technology* **60**, 601-610. [CrossRef]
33. Elena Bassoli, Andrea Gatto, Luca Iuliano. 2012. Joining mechanisms and mechanical properties of PA composites obtained by selective laser sintering. *Rapid Prototyping Journal* **18**:2, 100-108. [Abstract] [Full Text] [PDF]
34. R.D. Goodridge, C.J. Tuck, R.J.M. Hague. 2012. Laser sintering of polyamides and other polymers. *Progress in Materials Science* **57**, 229-267. [CrossRef]
35. K. Senthilkumaran, P.M. Pandey, P.V.M. Rao. 2012. Statistical modeling and minimization of form error in SLS prototyping. *Rapid Prototyping Journal* **18**:1, 38-48. [Abstract] [Full Text] [PDF]
36. Kristinn B. Gylfason, Andreas C. Fischer, B. Gunnar Malm, Henry H. Radamson, Lyubov M. Belova, Frank Niklaus. 2012. Process considerations for layer-by-layer 3D patterning of silicon, using ion implantation, silicon deposition, and selective silicon etching. *Journal of Vacuum Science & Technology B: Microelectronics and Nanometer Structures* **30**, 06FF05. [CrossRef]
37. Sung-Hoon Ahn, Jung-Oh Choi, Chung-Soo Kim, Gil-Yong Lee, Hyun-Taek Lee, Kyujin Cho, Doo-Man Chun, Caroline Sunyong Lee. 2012. Laser-assisted nano particle deposition system and its application for dye sensitized solar cell fabrication. *CIRP Annals - Manufacturing Technology* **61**, 575-578. [CrossRef]
38. Tatsuaki Furumoto, Mohd Rizal Alkahari, Takashi Ueda, Mohd Sanusi Abdul Aziz, Akira Hosokawa. 2012. Monitoring of Laser Consolidation Process of Metal Powder with High Speed Video Camera. *Physics Procedia* **39**, 760-766. [CrossRef]
39. Tatsuaki Furumoto, Takashi Ueda, Toru Amino, Akira Hosokawa. 2011. A study of internal face finishing of the cooling channel in injection mold with free abrasive grains. *Journal of Materials Processing Technology* **211**, 1742-1748. [CrossRef]
40. Chunze Yan, Liang Hao, Lin Xu, Yusheng Shi. 2011. Preparation, characterisation and processing of carbon fibre/polyamide-12 composites for selective laser sintering. *Composites Science and Technology* **71**, 1834-1841. [CrossRef]
41. Chen-Nan Sun, Mool C. Gupta, E. Andrew Payzant. 2011. Effect of Laser Sintering on Ti-ZrB 2 Mixtures. *Journal of the American Ceramic Society* **94**, 3282-3285. [CrossRef]
42. Zhixiang Cai, K.C. Yung, Xiaoyan Zeng. 2011. Fabrication and adhesion performance of gold conductive patterns on silicon substrate by laser sintering. *Applied Surface Science* **258**, 478-481. [CrossRef]
43. B. Gorny, T. Niendorf, J. Lackmann, M. Thoene, T. Troester, H.J. Maier. 2011. In situ characterization of the deformation and failure behavior of non-stochastic porous structures processed by selective laser melting. *Materials Science and Engineering: A* **528**, 7962-7967. [CrossRef]
44. Chen-Nan Sun, Mool C. Gupta, Wallace D. Porter. 2011. Thermophysical Properties of Laser-Sintered Zr-ZrB2 Cermets. *Journal of the American Ceramic Society* **94**:10.1111/jace.v94.8, 2592-2599. [CrossRef]
45. William Cooke, Rachel Anne Tomlinson, Richard Burguete, Daniel Johns, Gaëlle Vanard. 2011. Anisotropy, homogeneity and ageing in an SLS polymer. *Rapid Prototyping Journal* **17**:4, 269-279. [Abstract] [Full Text] [PDF]
46. Chunze Yan, Yusheng Shi, Jingsong Yang, Jinhui Liu. 2010. Investigation into the selective laser sintering of styrene–acrylonitrile copolymer and postprocessing. *The International Journal of Advanced Manufacturing Technology* **51**, 973-982. [CrossRef]

47. Joohan Kim, JeongU Rho, Jong Hyeong Kim. 2010. Laser solidification of conductive composites on a fabric surface. *Surface and Coatings Technology* **205**, 1812-1819. [CrossRef]
48. Myong-Ki Kim, Heui-Seok Kang, Kyung-Tae Kang, Sang-Ho Lee, Jun-Young Hwang, Seung-Jae Moon. 2010. Laser Sintering of Inkjet-Printed Silver Lines on Glass and PET Substrates. *Transactions of the Korean Society of Mechanical Engineers B* **34**, 975-982. [CrossRef]
49. Florencia Edith Wiria, Kah Fai Leong, Chee Kai Chua. 2010. Modeling of powder particle heat transfer process in selective laser sintering for fabricating tissue engineering scaffolds. *Rapid Prototyping Journal* **16**:6, 400-410. [Abstract] [Full Text] [PDF]
50. Prashant K. Jain, Pulak M. Pandey, P.V.M. Rao. 2010. Tailoring material properties in layered manufacturing. *Materials & Design* **31**, 3490-3498. [CrossRef]
51. Lino Costa, Deepak Rajput, Kathleen Lansford, Wenqiang Yue, Alexander Terekhov, William Hofmeister. 2010. The tower nozzle solid freeform fabrication technique. *Rapid Prototyping Journal* **16**:4, 295-301. [Abstract] [Full Text] [PDF]
52. Yuwen Zhang, Piyasak Damronglerd, Mo Yang. 2010. Analysis of Infiltration, Solidification, and Remelting of a Pure Metal in Subcooled Porous Preform. *Heat Transfer Engineering* **31**, 555-563. [CrossRef]
53. Yang Tong, Yao Shan, Zeng Feng. 2010. Profile invalidation approaching rapid prototyping. *Rapid Prototyping Journal* **16**:2, 146-155. [Abstract] [Full Text] [PDF]
54. I.A. Roberts, C.J. Wang, R. Esterlein, M. Stanford, D.J. Mynors. 2009. A three-dimensional finite element analysis of the temperature field during laser melting of metal powders in additive layer manufacturing. *International Journal of Machine Tools and Manufacture* **49**, 916-923. [CrossRef]
55. Rodger Blum, Pal Molian. 2009. Liquid-phase sintering of nanodiamond composite coatings on aluminum A319 using a focused laser beam. *Surface and Coatings Technology* **204**, 1-14. [CrossRef]
56. Tatsuaki Furumoto, Takashi Ueda, Naoto Kobayashi, Abdullah Yassin, Akira Hosokawa, Satoshi Abe. 2009. Study on laser consolidation of metal powder with Yb:fiber laser—Evaluation of line consolidation structure. *Journal of Materials Processing Technology* **209**, 5973-5980. [CrossRef]
57. Lino Costa, Rui Vilar. 2009. Laser powder deposition. *Rapid Prototyping Journal* **15**:4, 264-279. [Abstract] [Full Text] [PDF]
58. Rohan Kelkar. 2009. Laser sintering of conductive carbon paste on plastic substrate. *Optical Engineering* **48**, 074301. [CrossRef]
59. Prashant K. Jain, Pulak M. Pandey, P. V. M. Rao. 2009. Effect of delay time on part strength in selective laser sintering. *The International Journal of Advanced Manufacturing Technology* **43**, 117-126. [CrossRef]
60. Bettina Wendel, Dominik Rietzel, Florian Kühnlein, Robert Feulner, Gerrit Hülder, Ernst Schmachtenberg. 2008. Additive Processing of Polymers. *Macromolecular Materials and Engineering* **293**:10.1002/mame.v293:10, 799-809. [CrossRef]
61. Prashant K. Jain, Pulak M. Pandey, P.V.M. Rao. 2008. Experimental investigations for improving part strength in selective laser sintering. *Virtual and Physical Prototyping* **3**, 177-188. [CrossRef]
62. Y. Zhang, L. Hao, M. M. Savalani, R. A. Harris, K. E. Tanner. 2008. Characterization and dynamic mechanical analysis of selective laser sintered hydroxyapatite-filled polymeric composites. *Journal of Biomedical Materials Research Part A* **86A**:10.1002/jbm.a.v86a:3, 607-616. [CrossRef]
63. Jung-Woo Rho, Joo-Han Kim, Chul-Ku Lee. 2008. An Overview of Selective Laser Sintering. *Journal of the Korean Welding and Joining Society* **26**, 34-37. [CrossRef]
64. Omer Cansizoglu, Ola L.A. Harrysson, Harvey A. West II, Denis R. Cormier, Tushar Mahale. 2008. Applications of structural optimization in direct metal fabrication. *Rapid Prototyping Journal* **14**:2, 114-122. [Abstract] [Full Text] [PDF]
65. L-E. Rännar, A. Glad, C-G. Gustafson. 2007. Efficient cooling with tool inserts manufactured by electron beam melting. *Rapid Prototyping Journal* **13**:3, 128-135. [Abstract] [Full Text] [PDF]
66. J. H. Liu, Y. S. Shi, K. H. Chen, S. H. Huang. 2007. Research on manufacturing Cu matrix Fe-Cu-Ni-C alloy composite parts by indirect selective laser sintering. *The International Journal of Advanced Manufacturing Technology* **33**, 693-697. [CrossRef]
67. N. Raghunath, Pulak M. Pandey. 2007. Improving accuracy through shrinkage modelling by using Taguchi method in selective laser sintering. *International Journal of Machine Tools and Manufacture* **47**, 985-995. [CrossRef]
68. J.-P. Kruth, G. Levy, F. Klocke, T.H.C. Childs. 2007. Consolidation phenomena in laser and powder-bed based layered manufacturing. *CIRP Annals - Manufacturing Technology* **56**, 730-759. [CrossRef]
69. Alida Mazzoli, Giacomo Moriconi, Marco Giuseppe Pauri. 2007. Characterization of an aluminum-filled polyamide powder for applications in selective laser sintering. *Materials & Design* **28**, 993-1000. [CrossRef]
70. J.H. Liu, Y.S. Shi, Z.L. Lu, Y. Xu, K.H. Chen, S.H. Huang. 2007. Manufacturing metal parts via indirect SLS of composite elemental powders. *Materials Science and Engineering: A* **444**, 146-152. [CrossRef]
71. H. Zarringhalam, N. Hopkinson, N.F. Kamperman, J.J. de Vlieger. 2006. Effects of processing on microstructure and properties of SLS Nylon 12. *Materials Science and Engineering: A* **435-436**, 172-180. [CrossRef]

72. Edson Costa Santos, Masanari Shiomi, Kozo Osakada, Tahar Laoui. 2006. Rapid manufacturing of metal components by laser forming. *International Journal of Machine Tools and Manufacture* **46**, 1459-1468. [CrossRef]
73. L Hao, M M Savalani, Y Zhang, K E Tanner, R A Harris. 2006. Effects of material morphology and processing conditions on the characteristics of hydroxyapatite and high-density polyethylene biocomposites by selective laser sintering. *Proceedings of the Institution of Mechanical Engineers, Part L: Journal of Materials: Design and Applications* **220**, 125-137. [CrossRef]
74. U. Ajoku, N. Saleh, N. Hopkinson, R. Hague, P. Erasenthiran. 2006. Investigating mechanical anisotropy and end-of-vector effect in laser-sintered nylon parts. *Proceedings of the Institution of Mechanical Engineers, Part B: Journal of Engineering Manufacture* **220**, 1077-1086. [CrossRef]
75. Uzoma Ajoku, Neil Hopkinson, Mike Caine. 2006. Experimental measurement and finite element modelling of the compressive properties of laser sintered Nylon-12. *Materials Science and Engineering: A* **428**, 211-216. [CrossRef]